Coating prediction from reference cells measurements and eventual assistance of the UEP

E.S. Diaz & R.A. Adey
C.M. BEASY Ltd, UK.

Abstract

Damages appear on a hull of a vessel during its lifetime. In many cases the correct position of these damages are completely unknown. Its knowledge is important from mainly two points of view.

- Cathodic protection of the vessel. A corroded hull would be economically inefficient (current and fuel consumption) apart from being potentially dangerous since it is a hot point for crack corrosion [1].
- Noisiness of the vessel. Damages will increase the current flux from the anode to the cathode (damaged areas). This will augment the noise of the vessel and therefore it will become easily detectable to the enemy [2–4].

The aim of this work is to detect the damage by using the information available from the ICCP system and/or the signature.

1 Introduction

A vessel can be detected from its surrounding magnetic fields. This is due to two main sources:

- The magnetic field associated with the permanent/induced magnetism, present because of the material used in the construction of a vessel and the earth's magnetic field.
- The electrical currents driven by the ship into the sea. The principal sources of these currents are related with ship corrosion or the ICCP system. These magnetic fields are named Corrosion Related Magnetic Fields (CRM). The CRM can be a significant proportion of a ship's magnetic signature for vessels constructed using non-magnetic materials [5].

WIT Transactions on State of the Art in Science and Engineering, Vol 7, © 2005 WIT Press
www.witpress.com, ISSN 1755-8336 (on-line)
doi:10.2495/1-85312-889-9/07

Modelling techniques normally start from an assumed condition of the vessel. Given some assumed condition, the level of protection provided by the cathodic protection system can be predicted as well as the corrosion related electric and magnetic fields. Therefore, designers when assessing the signature and the effectiveness of the CP system will perform tests based on a number of possible conditions of the hull expected over the life cycle of the ship.

In typical CP systems, the designer knows the source of current (the anodes) but does not have a clear knowledge of where the current goes (the cathode) as this depends upon the condition of the metallic surfaces, *etc.* A method is therefore presented to determine where the current goes from the anodes and hence predict the general condition of the vessel and possible areas of damage. Once this information is known the associated electric and magnetic signatures can be predicted.

In addition, the detection of the areas of the vessel, which are acting as sinks of current, is of vital importance in order to know which part of the structure is disclosing the vessel. Their detection is a difficult matter that generally has to be solved in dry-docks by measuring the thickness of the coating with ultrasonic devices. However, to pull the ship out to the dry-dock to study the coating state is extremely costly. Moreover, on some occasions the area of the vessel which is taking current is concealed and cannot be easily detected even with the method indicated before.

In this chapter, the coating state of a structure, position and current taken by the damage, is analysed by using the information related with some sensors placed on the hull of the structure. The minimum amount of information necessary to carry out the prediction is searched for. Data will be presented showing the sensitivity of the predictions to the accuracy of the data and the number of reference cells, for example. Extra information of the Under Electric Potential (UEP) of the vessel will be included and their influence in the prediction will be shown.

Readers are advised that this paper can be viewed at the website <http://www.beasy.com/publications/paper/Predicting_Coating_Conditions.pdf> where the figures can be seen in their original colour format.

1.1 State of the art

In 1996, Aoki, Amaya and Gouka [6] applied the boundary element method to detect a paint defect on the hull of a ship. A painted hull with cathodic protection applied from some impressed anodes was studied, where the paint was assumed to be damaged during navigation. The damaged area could be accurately predicted with this method when the damage was located only on one element of the hull. However, the effectiveness of the method reduced significantly when the size of the damaged area was larger than an individual element. As the damaged size is unknown, the number of elements to use in the search is also unknown. A further complexity occurred where the damage had different coating thicknesses.

In a real case the unknowns are the following:

- The size of the damaged areas.
- The number of damaged areas.

- The position of the damaged areas.
- The coating thickness of the damaged areas.

This method could not cope with this amount of unknowns without carrying out a huge number of combinations.

In the approach proposed, an optimisation based search is performed to match the coating state of the surface. The predicted coating state is achieved by matching some potential reference data on the hull of the structure. Extra information, such as the Underwater Electric Potential (UEP) of the vessel, can also be included in the search. The quantity of information required, in particular the potential reference data, to obtain a reasonable solution is also studied.

1.2 Interpolation method

In order to identify the damaged areas, the coating of the vessel will be automatically modified by the optimisation method [7]. At least two polarisation curves should be considered, one with almost fully coated surface and the other with almost fully uncoated surface, representing the material underlying the coating. Once the value of the coating is found amongst the curves, a simple interpolation will provide the correct value of the current and potential.

The accuracy of the polarisation curve is an important factor in the simulation of a cathodic protection problem if accurate predictions are to be made of the protection potential and the current. However, in this case, an accurate polarisation curve of the underlying material was found not to be needed. This conclusion was obtained after using a linear polarisation curve to predict the state of the coating. A possible explanation for this unexpected result is that in the models solved, the ship hull was normally considered to be coated with a 'perfect paint' except in the areas where there was damage. Therefore the polarisation curve was simply used to differentiate between areas of the hull where the current flow into the hull was zero (the perfectly painted areas) and the areas where there was current flow into the hull (the damaged areas). Further studies would be necessary to test this hypothesis for cases where the general condition of the hull required different percentages of coating damages.

Nevertheless, successful results were obtained using realistic polarisation data as well.

The term coating sensors will be employed, from now on, as point positions on the surface of the hull at which the coating will be modified (fig. 6) by the optimisation surface (variables). The coating of the rest of the surface will be interpolated amongst these coating sensors. Two methods of interpolation were investigated, Radial Basis functions and three closest coating sensors.

1.2.1 Radial Basis function interpolation

Radial basis functions (RBFs) are a class of functions that exhibit radial symmetry, that is, they may be seen to depend only, apart from some known parameters, on the distance $r = \| x - x_j \|$ between the centre of the function and a generic point x. These functions can be generically represented in the form $\phi(r)$. This means that there exist infinite radial basis functions [8].

These functions may be classed into: globally supported and compactly supported ones depending on their supports, this is to say, whether they are defined on the whole domain or only on part of it.

Those most employed within the globally supported RBFs are:

$$\text{Multiquadratic(MQ)} \quad \sqrt{(x - x_j)^2 + c_j^2}\,,\ c_j > 0 \tag{1}$$

$$\text{Reciprocal Multiquadratic (RMQ)} \quad \left((x - x_j)^2 + c_j^2\right)^{-1/2},\ c_j > 0 \tag{2}$$

$$\text{Gaussians (G)} \quad \exp\left(-cr^2\right),\ c_j > 0 \tag{3}$$

$$\text{Thin-plate splines (TPS)} \quad r^{2\beta} \ln r, \beta \in M \tag{4}$$

Where:

c is a coefficient.
M is an integer number.

Within the compactly supported RBFs are:
Wu and Wendland,

$$(1-r)^t + q(r) \tag{5}$$

Where:

q(r) is a polynomial and $(1-r)^t$ is 0 for r greater than the support.
t is the polynomial order of $(1-r)^t$

Buhmann,

$$\frac{1}{3} + r^2 - \frac{4}{3} r^3 + 2r^2 \ln r \tag{6}$$

The previous RBFs were attempted for the problem of predicting the coating using coating sensors points. The best predictions were achieved by the equation shown below:

$$(1-r)^2 \tag{7}$$

Briefly, an interpolation with RBFs may take the form:

$$s(p) = \sum_{j=1}^{N} \alpha_j \varphi\left(\left\|p - p_j\right\|\right) \tag{8}$$

In this case:

$$s(p) = \sum_{j=1}^{N} \alpha_j (1-r)^2 = \sum_{j=1}^{N} \alpha_j \left(1 - \|p - p_j\|\right)^2 \tag{9}$$

Where:

N is the number of generic points.
p is the generic point.

The values of s(p) are known, coating values, and therefore the set of equations of the form:

$$s(p_1) = \sum_{j=1}^{N} \alpha_j \left(1 - \|p_1 - p_j\|\right)^2 \tag{10}$$

$$s(p_2) = \sum_{j=1}^{N} \alpha_j \left(1 - \|p_2 - p_j\|\right)^2 \tag{11}$$

$$s(p_N) = \sum_{j=1}^{N} \alpha_j \left(1 - \|p_N - p_j\|\right)^2 \tag{12}$$

The α_j parameters are obtained by solving the above system of equations.

Once the α_j are found, eqn (9) can be applied to all the points of the surface.

The generic points are our coating sensors points, which are the variables of the optimisation.

1.2.2 Three closest coating sensors

The three closest coating sensors can be employed to compute the coating of the current point by using a linear interpolation.

The process is based on the next steps:

1. The three closest coating sensors to the point considered, *i*, are searched for; their coating values, $s(p_1)$, $s(p_2)$, $s(p_3)$, and their distances to the considered point, d_{i1}, d_{i2}, d_{i3}, are taken.
2. The equivalent distance (d_{eq}) is computed.

$$\frac{1}{d_{eq}} = \frac{1}{d_{i1}} + \frac{1}{d_{i2}} + \frac{1}{d_{i3}} \tag{13}$$

3. And the value of the coating at the point considered is computed:

$$s(p_i) = \frac{d_{eq}}{d_{i1}} s(p_1) + \frac{d_{eq}}{d_{i2}} s(p_2) + \frac{d_{eq}}{d_{i3}} s(p_3) \tag{14}$$

The eqns (9) and (14) were used to predict the coating of the surface, Radial Basis Functions behaved slightly better than the three closest coating sensors. Thus, RBFs was the method of interpolation selected to implement the experi ments below. Some additional experiments are implemented with the three closest coating sensors at the end of this chapter.

1.3 Prediction of the coating from reference cells measurements, objective function and constraints

The optimisation process requires the problem posed in the form of an objective function, design variables and constraints. The objective function was defined as the sum of the squares of the difference between the target potentials at the reference cells and the potentials predicted by the model (15) in order to match the measured reference cell potentials.

$$\text{Obj}= \sum_{i=1}^{i=n} \left(V_{t_i} - V_i\right)^2 \tag{15}$$

Subject to the following constraints on the surface of the cathode:

$$g_i= \frac{V_i - V_{max,i}}{\left|V_{min,i}\right|} \le 0 \text{ on } \Gamma_C \quad i= 1,\ldots,m \tag{16}$$

$$g_j= \frac{V_{min,j} - V_j}{\left|V_{min,j}\right|} \le 0 \text{ on } \Gamma_C \quad j= 1,\ldots,m \tag{17}$$

Where:

n is the number of references cells potential.
V_t is the target potential at the reference cell.
V_{min} is the minimum potential required at a reference cell.
V_{max} is the maximum potential required at a reference cell.
V is the computed potential at a reference cell.
Γ_C is the surface of the cathode.
m is the number of elements on the surface.

Note: It is normally recommended for the optimisation algorithms [9] that to obtain a well-conditioned problem the constraints will have roughly the same order of magnitude as the gradients (within a factor of 100). Therefore, the denominator of eqns (16) and (17) were applied to scale the constraints into non-dimensional units.

The constraints were applied to limit the search space to that of practical significance with the resulting benefit that the speed of the solution was improved.

The method of optimisation used was the Sequential Linear Programming (SLP) which is a *Multivariable search* method [9]. This procedure uses algorithms which are based on geometric or logical concepts to move rapidly from a starting point away from the optimum to a point near the optimum. In addition, they attempt to satisfy the constraints associated with the problem and the Kuhn-Tucker conditions [10] as they generate improved values of the model.

1.4 The models

Two models were used to check whether the prediction of the coating was accurate, a cylinder model and a frigate model.

1.4.1 Cylinder model, description

A model of a cylinder was considered to study the prediction of the coating state.

The dimensions of the cylinder are:

- Length: 34.0m.
- Diameter: 10.0m.

The model has the characteristics shown in fig. 1. The surface of the cylinder was considered fully coated, thus, no current leaked through its surface apart from the damaged areas studied in the experiments. The surface near one of the edges of the cylinder was set of being made of Nickel-Aluminium-Bronze.

The electrolyte considered was seawater with a resistivity of 20ohm·cms [11], that implies a conductivity of about 5S/m.

To speed up the solution and since the model is symmetric, only half of it was modelled. The model has 619 elements, including the surrounding box which simulates the electrolyte. The cylinder itself was modelled with 600 elements.

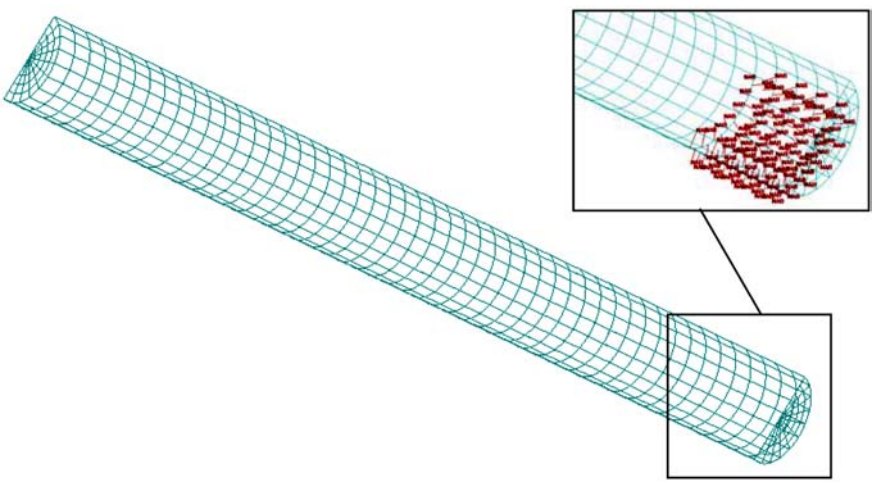

Figure 1: Cylinder model with Nickel-Aluminium-Bronze area. (Coloured versions of figure 1 and subsequent figures can be viewed at http://www.beasy.com/publications/papers/Predicting_Coating_Conditions.pdf).

1.4.2 Frigate model, description

A model of a frigate model was also considered to study the prediction of the coating state. The model has the characteristics shown in fig. 2. The frigate was considered fully coated apart from some specific damaged areas. The propeller was set made of nickel-aluminium-bronze.

To speed up the solution, and since the model is symmetric, only half of it was modelled.

The electrolyte considered was seawater with a resistivity of 20ohm·cms [11], that implies a conductivity of about 5S/m.

From the modelling perspective, the model has 1738 elements, including the surrounding box which simulates the electrolyte. The frigate itself was modelled with 1338 elements in most of the experiments analysed. A more refined mesh was created at the stern of the vessel since it is the most critical area of the frigate due to the propeller and location of the main anodes.

1.5 Cylinder model

Several sets of coating sensors were placed on the cylinder surface model (1.4.1) to study the effectiveness of the method. The potential data of the reference cells are to be added one by one to the optimisation to study their influence in the prediction of the coating state.

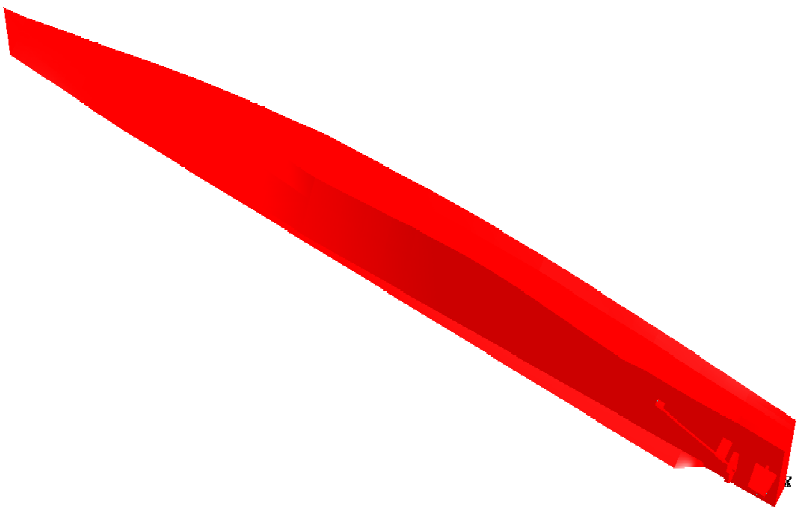

Figure 2: Frigate model. The dimensions of the frigate are:

- Waterline length: 34.0m.
- Draft: 2.3m.
- Waterline beam: 6.4m.

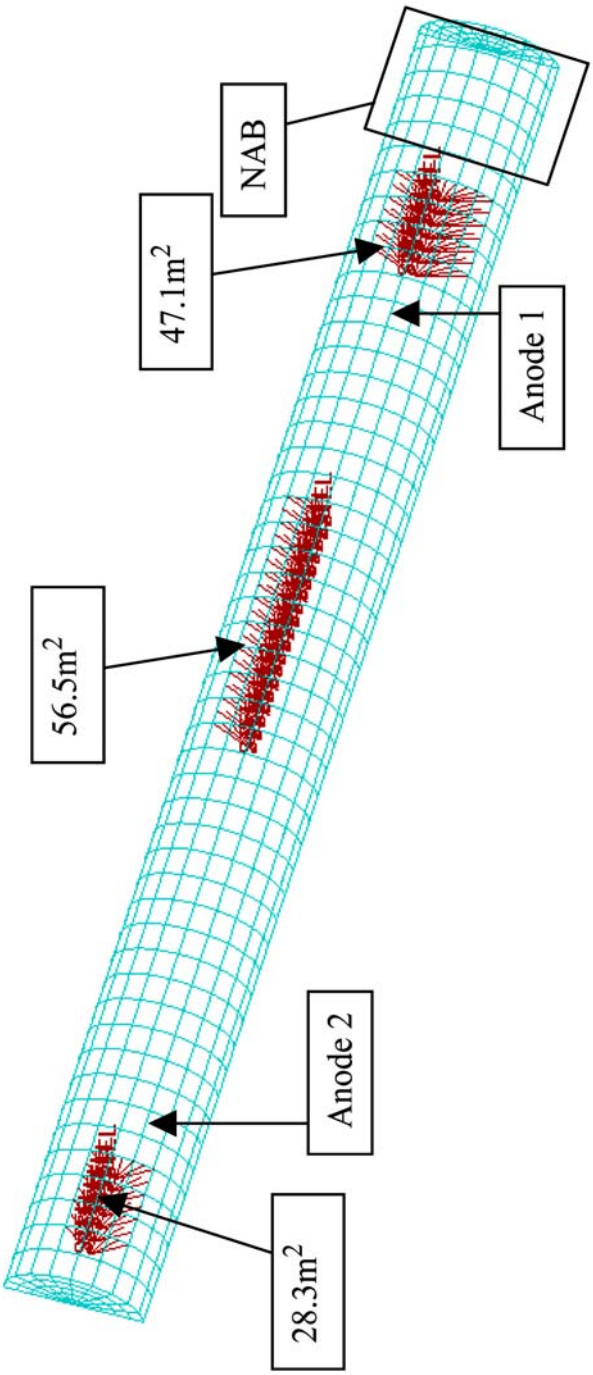

Figure 3: Damaged areas placed on the cylinder surface.

Table 1: Current at the anodes.

	Current Density (mA/m^2)	Current (mA)
Anode 1	–6903.0	–21687.4
Anode 2	–4455.0	–13995.8

1.5.1 Damaged areas

Three damaged areas, bare steel, were placed on the cylinder surface. Figure 3 shows the position and size of the damaged areas.

1.5.2 Currents and positions of the anodes

Two impressed anodes were placed on the surface of the model (fig. 3). The currents supplied by each one of the anodes are shown in the table 1.

1.5.3 Coating search area

Figure 4 shows the search area in which the damaged areas are to be predicted.

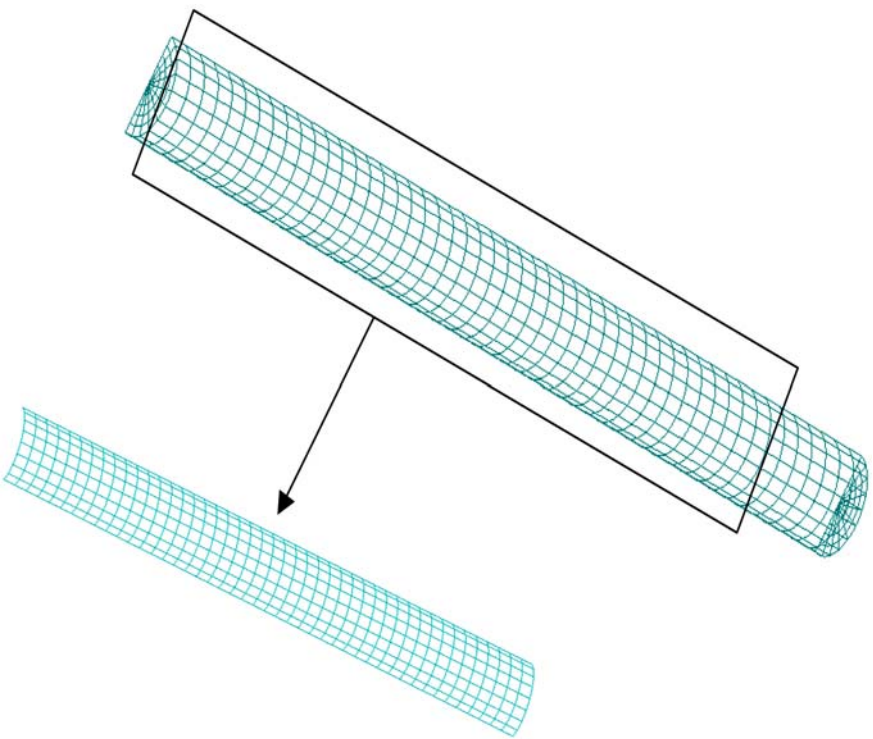

Figure 4: Search area on the cylinder structure.

Table 2: Target and constraints for five reference cells.

	Target (mV)	Constraint (mV)
REF1	–802.5	–770, –777
REF2	–788.5	–765, –775
REF3	–779.2	–755, –762
REF4	–828.5	–864, –870
REF5	–820.1	–815, –820

1.5.4 Reference cells
The number of reference cells, target values, was increased to determine how much data was required to detect the damage.

Figure 5 shows the position of the reference cells on the cylinder surface.

Tight constraints were set around the target values to make the optimisation software reach the target with more accuracy. The constraint values applied are shown in table 2.

1.5.5 First array of coating sensors, 7 coating sensors
An array of 7 coating sensors was placed on the predicting surface, distributed as it is shown in fig. 6. A radial basis function was employed as interpolation function to emulate the real state of the surface.

1.5.5.1 One reference cell The first reference cell potential was used as target value on the optimisation process (fig. 5).

Table 3 shows that only one damaged area at the edge of the search surface was found. There is not enough information to represent the real state of the surface since the constraints, despite being reasonably tight, are satisfied and the objective function presents a small value.

1.5.5.2 Two reference cells The second reference cell potential is added as target value on the optimisation process (fig. 5).

Table 4 shows that two damaged areas at the edges of the search surface were found. There is not enough information to represent the real state of the surface since the constraints, despite being reasonably tight, are satisfied. The objective function presents a higher value since the optimisation algorithm finds it difficult to match the sum of least squares and satisfy the constraints.

1.5.5.3 Three reference cells The third reference cell potential is added as target value on the optimisation process (fig. 5).

Table 5 shows that still only two of the three damaged areas are revealed. Again there is not enough information to represent the real state of the surface since while the constraints are satisfied, the objective function gives a high value.

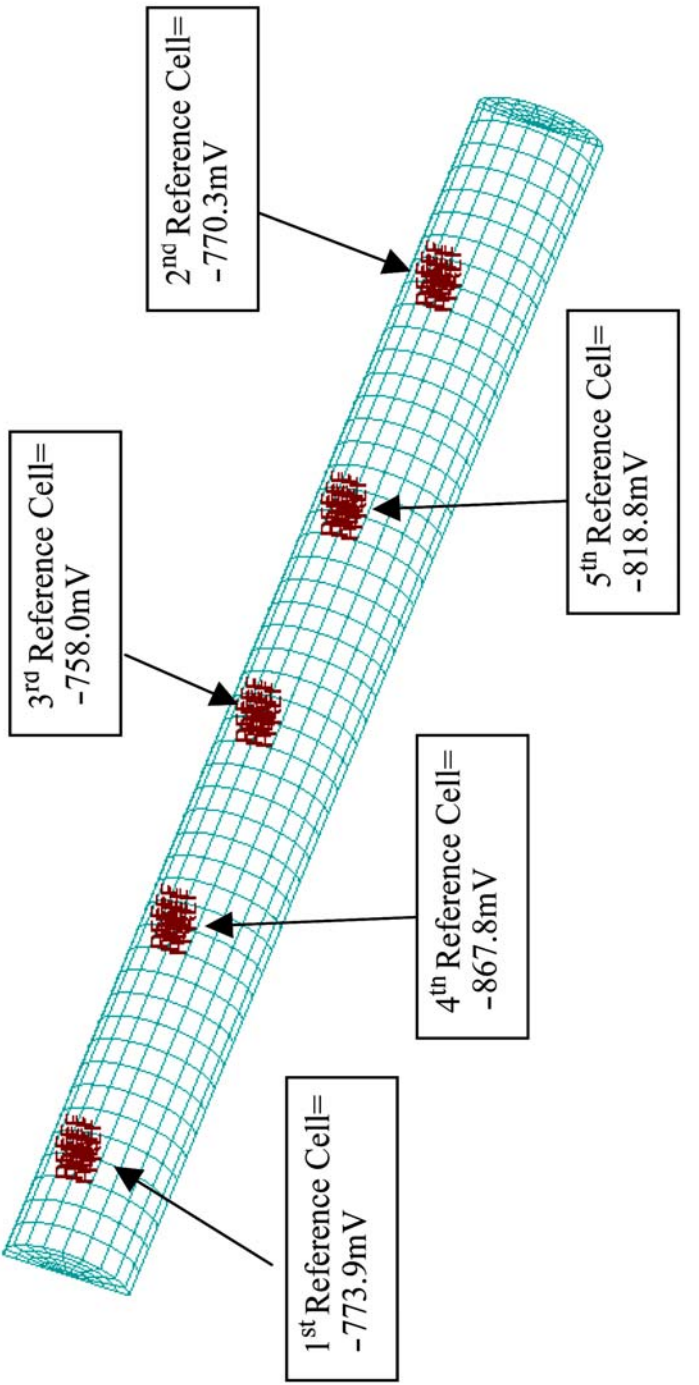

Figure 5: Position of the five reference cells on the cylinder surface.

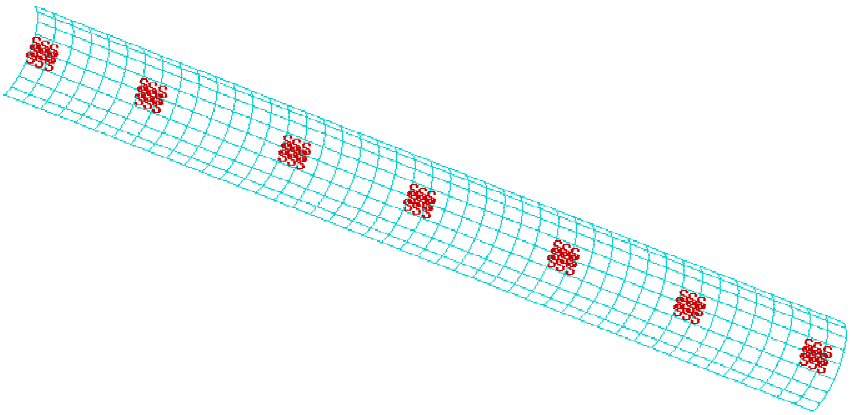

Figure 6: Seven coating sensors distribution on the prediction surface.

Table 3: Summary of results obtained when one reference cell was used as target value and 7 coating sensors to emulate the coating.

One reference cell	
	7 Coating sensors
Iterations	10
Objective function (mV^2)	0.038
Number of references in the constraints	1/1
SURFACE REF1: Potential (mV)	–773.7
Absolute error target, 1st Ref Cell (mV)	0.2
Display	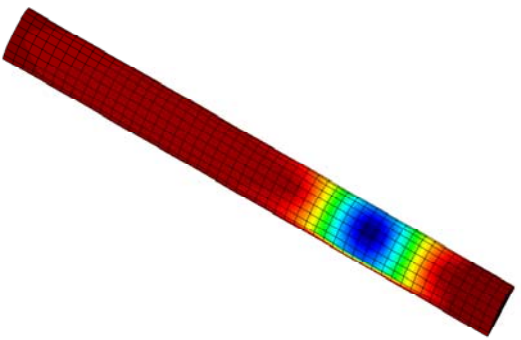

Table 4: Summary of results obtained when two reference cells were used as target value and 7 coating sensors to emulate the coating.

Two reference cells	
	7 Coating sensors
Iterations	9
Objective function (mV^2)	4.779
Number of references in the constraints	2/2
SURFACE REF1: Potential (mV)	–773.6
SURFACE REF2: Potential (mV)	–768.1
Absolute error target, 1st Ref Cell (mV)	0.3
Absolute error target, 2nd Ref Cell (mV)	2.2
Display	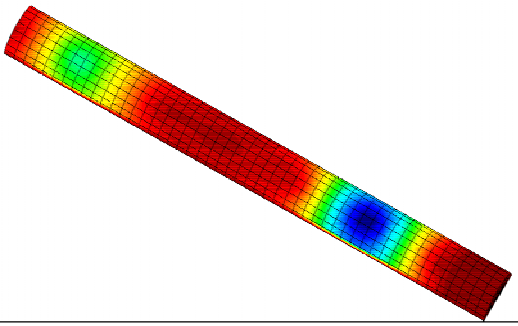

1.5.5.4 Four reference cells The fourth reference cell potential is added as target value on the optimisation process (fig. 5).

In this case, table 6 shows that three damaged areas were found in an approximate correct position (fig. 3). The constraints are not satisfied due to the tight constraints around the target values. However, the optimisation tried to match them. Consequently, the final solution is the best solution which minimises the objective function and approaches the constraints.

1.5.5.5 Five reference cells The fifth reference cell potential is added as target value on the optimisation process (fig. 5).

In this case, table 7 shows that three damaged areas were also found in an approximate correct position (fig. 3). As previously, the constraints are not satisfied due to the tight constraints around the target values. However, the optimisation tried to match them. Consequently, the final solution is the best solution that minimises the objective function and approaches the constraints.

Table 5: Summary of results obtained when three reference cells were used as target value and 7 coating sensors to emulate the coating.

Three reference cells	
	7 Coating sensors
Iterations	6
Objective function (mV^2)	47.6
Number of references in the constraints	2/3
SURFACE REF1: Potential (mV)	–771.8
SURFACE REF2: Potential (mV)	–765.1
SURFACE REF3: Potential (mV)	–762.0
Absolute error target, 1st Ref Cell (mV)	2.1
Absolute error target, 2nd Ref Cell (mV)	5.2
Absolute error target, 3rd Ref Cell (mV)	4.0
Display	

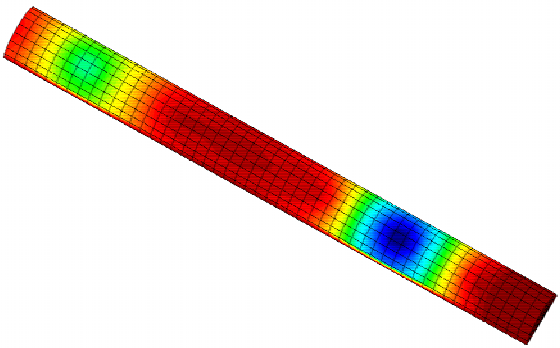

Two more sets of coating sensors (9 coating sensors and 20 coating sensors) where studied obtaining similar results to this first set of coating sensors.

1.5.6 Tests with 9 and 20 Coating sensors

A second and third array of 9 and 20 coating sensors were placed on the model (fig. 7). A set of tests were performed similar to that described earlier where the number of reference cell measurements were increased until the damage pattern was identified.

Table 6: Summary of results obtained when four reference cells were used as target value and 7 coating sensors to emulate the coating.

Four reference cells	
	7 Coating sensors
Iterations	4
Objective function (mV^2)	3171.2
Number of references in the constraints	0/4
SURFACE REF1: Potential (mV)	−802.0
SURFACE REF2: Potential (mV)	−787.4
SURFACE REF3: Potential (mV)	−772.0
SURFACE REF4: Potential (mV)	−824.3
Absolute error target, 1st Ref Cell (mV)	28.1
Absolute error target, 2nd Ref Cell (mV)	17.1
Absolute error target, 3rd Ref Cell (mV)	14.0
Absolute error target, 4th Ref Cell (mV)	43.5
Display	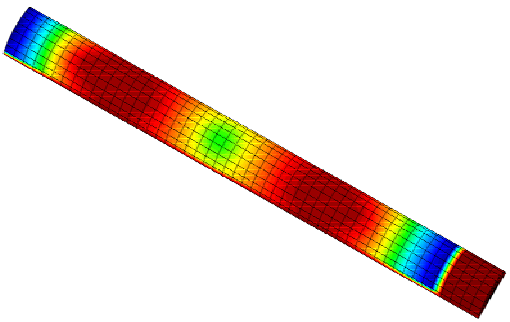

1.5.6.1 One reference cell The first reference cell potential is used as target value (fig. 5)

1.5.6.2 Two reference cells The second reference cell potential is added as target (fig. 5).

1.5.6.3 Three reference cells The third reference cell potential is added as target value (fig. 5).

Table 7: Summary of results obtained when five reference cells were used as target values and 7 coating sensors to emulate the coating.

Five reference cells	
	7 Coating sensors
Iterations	4
Objective function (mV^2)	3171.2
Number of references in the constraints	0/4
SURFACE REF1: Potential (mV)	–802.5
SURFACE REF2: Potential (mV)	–788.5
SURFACE REF3: Potential (mV)	–779.2
SURFACE REF4: Potential (mV)	–828.5
SURFACE REF5: Potential (mV)	–820.1
Absolute error target, 1st Ref Cell (mV)	28.6
Absolute error target, 2nd Ref Cell (mV)	18.2
Absolute error target, 3rd Ref Cell (mV)	21.2
Absolute error target, 4th Ref Cell (mV)	39.3
Absolute error target, 5th Ref Cell (mV)	1.3
Display	

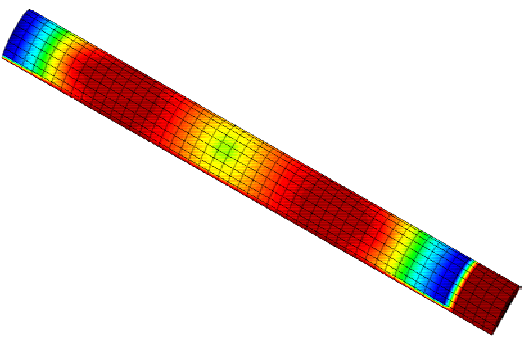

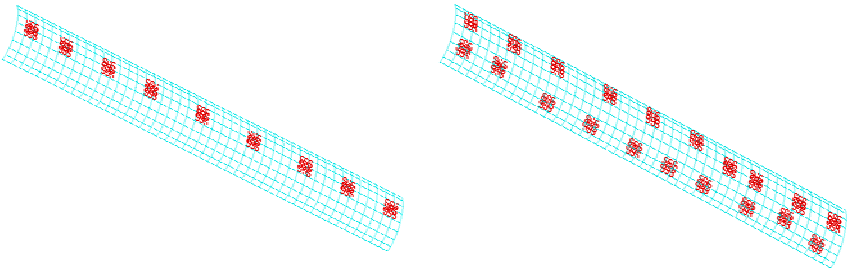

Figure 7: Nine and twenty coating sensors distribution on the prediction surface.

1.5.6.4 Four reference cells The fourth reference cell potential is added as target value (fig. 5).

1.5.6.5 Five reference cells The fifth reference cell potential is added as target value (fig. 5).

1.5.7 Summary, cylinder

The objective function increases its value with the number of reference cells, since the distribution of the coating sensors and the RBFs do not exactly represent the real situation on the damaged areas. Likewise, the constraint tolerance is not satisfied when the number of reference cells exceeds a certain number. The best results, in the experiment analysed, are obtained when the number of reference cells data is at least 4, regardless of the number of coating sensors. At that point, despite the constraint tolerance being exceeded, the results highlight the damaged areas and predicted the correct current flow in the model. The possible explanation for the good results being obtained is that the final design/solution is the best that could be achieved with the data provided. In general all the cases indicate that the more information available from the reference cells the better the prediction (table 13).

Table 8: Summary of results obtained when only one reference cell was used as target value with 9 and 20 coating sensors, respectively, to emulate the coating distribution.

One reference cell		
	9 Coating sensors	**20 Coating sensors**
Iterations	11	16
Objective function (mV^2)	0.81	0.06
Number of references in the constraints	1/1	1/1
SURFACE REF1: Potential (mV)	−773.0	−774.1
Absolute error target, 1st Ref Cell (mV)	0.9	0.2

Table 9: Prediction obtained when only one reference cell was used as target value with 9 and 20 coating sensors, respectively, to emulate the coating distribution.

	9 Coating sensors	**20 Coating sensors**
Display	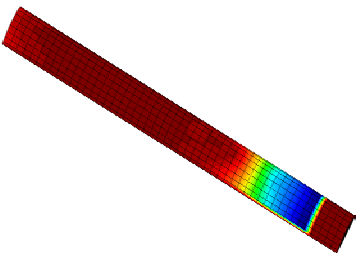	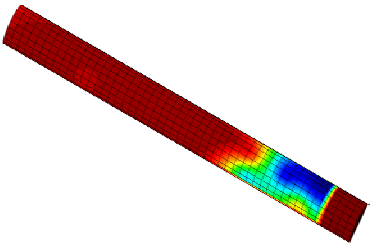

The constraints are satisfied when the number of reference cells is three or less but the solution does not completely predict all the damaged areas. However, when the number of reference cells is four or above the solution is clear but the constraints are not satisfied.

1.6 Frigate model

The frigate model was also considered to study the prediction of the coating state.

Two impressed anodes were placed on the surface of the model (Figure 8). The currents supplied by each one of the anodes are shown in the table 18.

Table 10: Summary of results obtained when two reference cells were used as target value with 9 and 20 coating sensors, respectively, to emulate the coating distribution.

Two reference cells		
	9 Coating sensors	**20 Coating sensors**
Iterations	11	11
Objective function (mV^2)	8.3	0.4
Number of references in the constraints	2/2	2/2
SURFACE REF1: Potential (mV)	−771.4	−773.7
SURFACE REF2: Potential (mV)	−768.8	−769.7
Absolute error target, 1st Ref Cell (mV)	2.5	0.2
Absolute error target, 2nd Ref Cell (mV)	1.5	0.6

Table 11: Prediction obtained when two reference cells were used as target value with 9 and 20 coating sensors, respectively, to emulate the coating distribution.

	9 Coating sensors	20 Coating sensors
Display	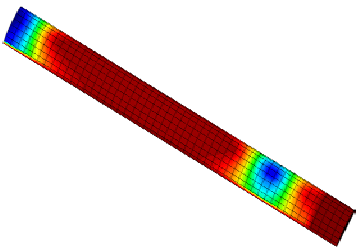	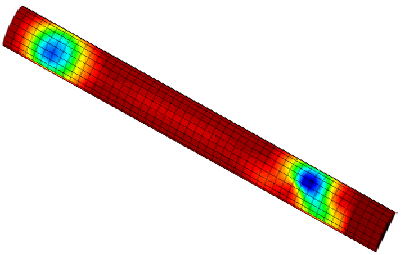

In order to test the methodology a test model was created by creating three areas of damage on the surface of the frigate, the model was solved and the results used to create the target data. Note that additional tests were performed to assess the impact of noise in the target data and other geometries. The results presented below are representative of those results.

The optimisation attempted to match the target model. An exact match will not be obtained because the damage was defined over discrete elements of the

Table 12: Summary of results obtained when three reference cells were used as target value with 9 and 20 coating sensors, respectively, to emulate the coating distribution.

Three reference cells		
	9 Coating sensors	**20 Coating sensors**
Iterations	19	16
Objective function (mV^2)	9.5	0.7
Number of references in the constraints	3/3	3/3
SURFACE REF1: Potential (mV)	–776.4	–773.9
SURFACE REF2: Potential (mV)	–772.0	–770.4
SURFACE REF3: Potential (mV)	–757.3	–757.2
Absolute error target, 1st Ref Cell (mV)	2.5	0.0
Absolute error target, 2nd Ref Cell (mV)	1.7	0.1
Absolute error target, 3rd Ref Cell (mV)	0.7	0.8

Table 13: Prediction obtained when three reference cells were used as target value with 9 and 20 coating sensors, respectively, to emulate the coating distribution.

	9 Coating sensors	**20 Coating sensors**
Display	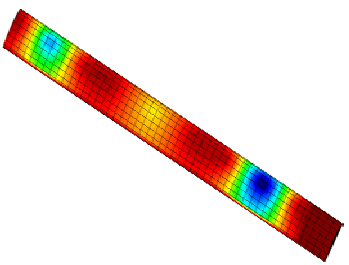	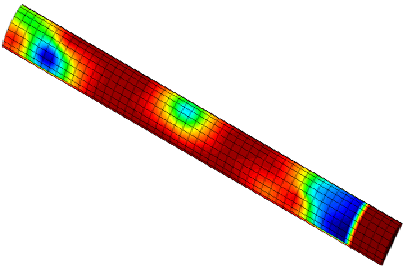

model whereas the coating sensors can only provide a general idea on the size and location of the damage.

Several sets of coating sensors were placed on the surface of the frigate model. Reference cells are to be included one by one in the process, as target values, to study their influence in the prediction of the coating.

Table 14: Summary of results obtained when four reference cells were used as target value with 9 and 20 coating sensors, respectively, to emulate the coating distribution.

Four reference cells		
	9 Coating sensors	**20 Coating sensors**
Iterations	4	17
Objective function (mV^2)	5253.4	2424.2
Number of references in the constraints	0/4	0/4
SURFACE REF1: Potential (mV)	−800.3	−797.3
SURFACE REF2: Potential (mV)	−830.1	−792.2
SURFACE REF3: Potential (mV)	−778.5	−777.0
SURFACE REF4: Potential (mV)	−844.1	−835.6
Absolute error target, 1st Ref Cell (mV)	26.4	23.4
Absolute error target, 2nd Ref Cell (mV)	59.8	21.9
Absolute error target, 3rd Ref Cell (mV)	20.5	19.0
Absolute error target, 4th Ref Cell (mV)	23.7	32.2

Table 15: Prediction obtained when four reference cells were used as target value with 9 and 20 coating sensors, respectively, to emulate the coating distribution.

	9 Coating sensors	20 Coating sensors
Display	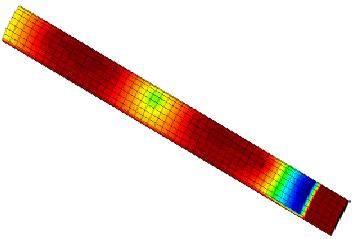	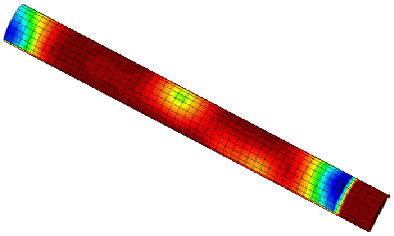

Table 16: Summary of results obtained when five reference cells were used as target value with 9 and 20 coating sensors, respectively, to emulate the coating distribution.

Five reference cells		
	9 Coating sensors	**20 Coating sensors**
Iterations	4	14
Objective function (mV^2)	6339.1	2538.7
Number of references in the constraints	0/5	1/5
SURFACE REF1: Potential (mV)	–804.1	–803.6
SURFACE REF2: Potential (mV)	–831.5	–779.1
SURFACE REF3: Potential (mV)	–790.4	–774.9
SURFACE REF4: Potential (mV)	–851.0	–831.8
SURFACE REF5: Potential (mV)	–837.3	–818.2
Absolute error target, 1st Ref Cell (mV)	30.2	29.7
Absolute error target, 2nd Ref Cell (mV)	61.2	8.8
Absolute error target, 3rd Ref Cell (mV)	19.0	16.9
Absolute error target, 4th Ref Cell (mV)	32.2	36.0
Absolute error target, 5th Ref Cell (mV)	5.5	0.6

Table 17: Prediction obtained when five reference cells were used as target value with 9 and 20 coating sensors, respectively, to emulate the coating distribution.

	9 Coating sensors	20 Coating sensors
Display	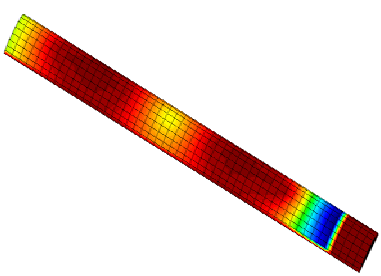	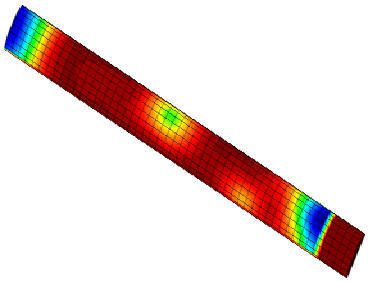

1.6.1 Damaged areas

Three damaged areas, bare steel, were placed on the surface of the frigate. Figure 8 shows the position and size of the damaged areas.

1.6.2 Coating sensors arrays

Two arrays of coating sensors were utilised in the frigate model, an array of 7 coating sensors and an array of 12 coating sensors distributed as shown in fig. 9.

A radial basis function was used to interpolate the data from the coating sensors on the hull surface.

1.6.3 Reference cells

The number of reference cells, target values, was increased to determine how much data was required to detect the damage.

Figure 10 shows the position of the reference cells on the hull surface.

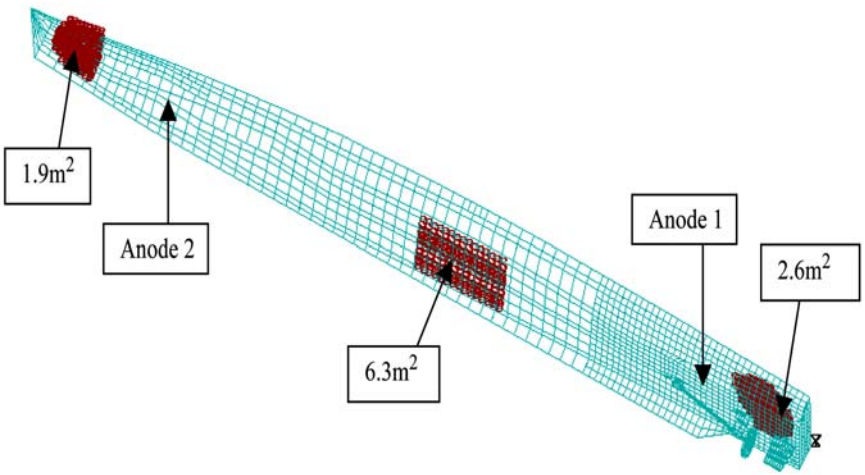

Figure 8: Damaged areas placed on the surface of the frigate and anodes position.

Table 18: Current at the anodes.

	Current Density (mA/m^2)	Current (mA)
Anode 1	−33554.1	−1813.7
Anode 2	−18262.1	−1649.9

Tight constraints were set around the target value to make the optimisation software reach the target with more accuracy. The constraint values applied are shown in table 19.

1.6.4 Frigate, results

The best results, in the experiment analysed, were obtained when the number of reference cells was at least 4. The final design clearly showed the damaged areas when four reference cells were used. The final design was still accurate but started to drift out of the range of constraints when the number of reference cells was above three.

The tables (table 20, table 21, table 22, table 23 and table 24) show how far the potential of each one of the surfaces studied are to the target one. The constraints are satisfied when the number of reference cells, target values, is three, two and one, but the solution is not complete. Some damaged areas are shown on the frigate hull, but other damaged areas are not shown yet since the information is insufficient.

When the number of reference cells is four or above the solution is clear. Increasing the number of coating sensors resulted in a reduction in the difference between the target potential and the final design potential.

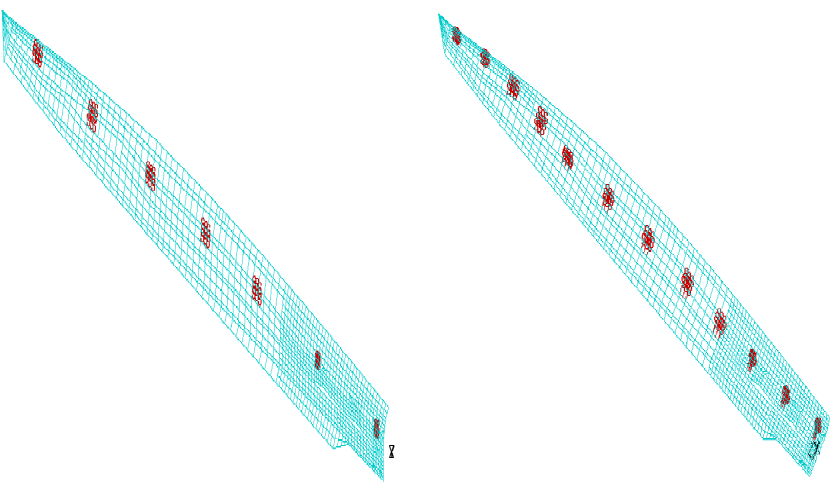

Figure 9: Seven and twelve coating sensors distribution on the surface of the frigate.

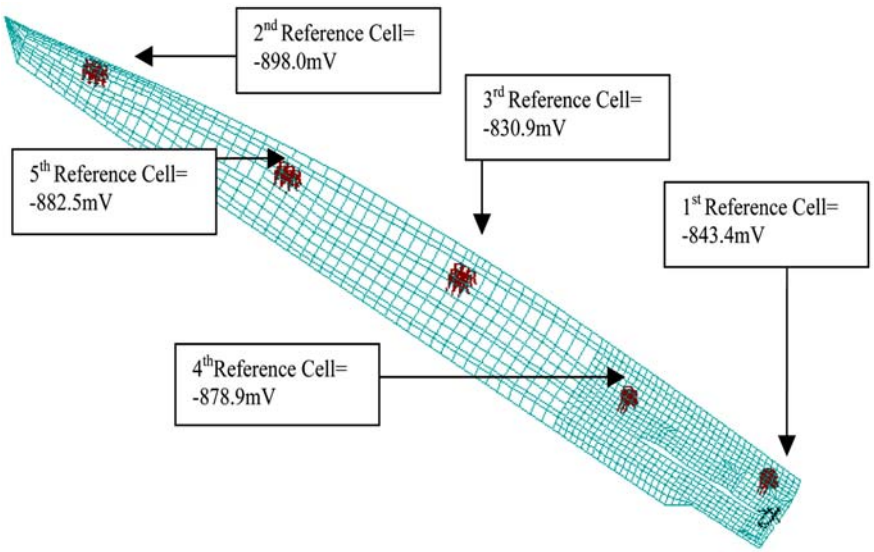

Figure 10: Position of the five reference cells on the hull surface of the frigate.

In the case with five reference cells, the solution obtained when the number of coating sensors was seven seems to be a better prediction than when the number of coating sensors was twelve. A possible explanation for this phenomenon is that the sensors in this case are placed closer to the bow of the frigate (fig. 9). Therefore, they are better able to represent the damage in that area. This assumption was confirmed with a new analysis carried out using only ten sensors (fig. 11 and fig. 12), removing the first and third sensors of the twelve previously had.

1.6.5 Summary, frigate

A frigate model has been analysed with three damaged areas on its surface. A compact radial basis function was used to interpolate the coating condition among the 'coating sensors'.

Table 19: Target and constraints for five reference cells.

	Target (mV)	Constraint (mV)
REF1	–843.4	–840, –850
REF2	–898.0	–895, –905
REF3	–830.9	–825, –835
REF4	–878.9	–873, –883
REF5	–882.5	–877, –887

Table 20: Results obtained using the 1st reference cell as target value and two different sets of arrays.

One reference cell		
	7 Coating sensors	**12 Coating sensors**
Iterations	13	11
Objective function (mV^2)	0.127	0.122
Number of references in the constraints	1/1	1/1
SURFACE REF1: Potential (mV)	−843.0	−843.7
Absolute error target, 1st Ref Cell (mV)	0.4	0.3
Display	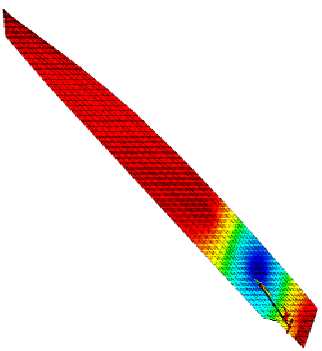	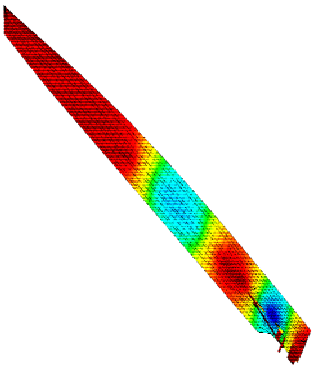

The number and position of reference cells, to determine where the damaged areas are, is not known in advance. In addition, a ship's ICCP system will be designed to provide the best ICCP system performance not necessarily to identify areas of damage. Consequently, if a reference cell is near a damaged area, the damage will be quickly predicted. However, reference cells placed away from the damaged areas will not give significant information unless the cells can provide an overall pattern sufficient to detect the damage. Therefore, in some cases the information provided is enough to predict, with accuracy, what the condition of the hull is, but in other occasions more information is needed. To avoid the uncertainty of this lack of information, several positions of the coating sensors should be studied. If the damaged areas appear consistently in the same area, then the damaged areas have been found.

Table 21: Results obtained using the 1st and the 2nd reference cell as target values and two different sets of arrays.

Two reference cells		
	7 Coating sensors	**12 Coating sensors**
Iterations	9	9
Objgective function (mV^2)	2.368	0.755
Number of references in the constraints	2/2	2/2
SURFACE REF1: Potential (mV)	–842.3	–843.1
SURFACE REF2: Potential (mV)	–897.1	–897.2
Absolute error target, 1st Ref Cell (mV)	1.10	0.30
Absolute error target, 2nd Ref Cell (mV)	0.90	0.80
Display		

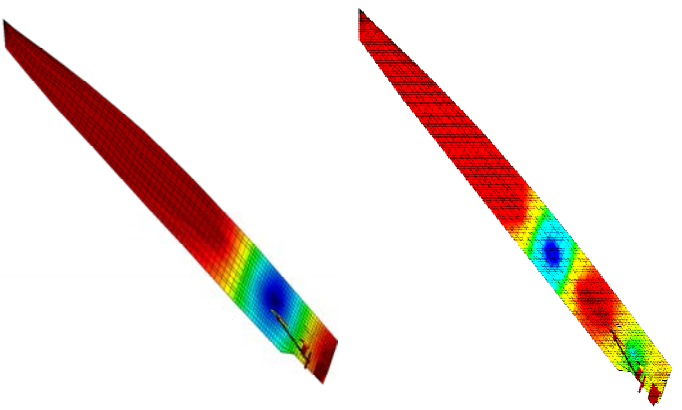

Table 22: Results obtained using the 1st, the 2nd and the 3rd references cell as target values and two different sets of arrays.

Three reference cells		
	7 Coating sensors	**12 Coating sensors**
Iterations	7	11
Objective function (mV^2)	40.255	2.79
Number of references in the constraints	3/3	3/3
SURFACE REF1: Potential (mV)	–843.1	–844.5
SURFACE REF2: Potential (mV)	–901.1	–898.5
SURFACE REF3: Potential (mV)	–825.4	–829.8
Absolute error target, 1st Ref Cell (mV)	0.30	1.10
Absolute error target, 2nd Ref Cell (mV)	3.10	0.50
Absolute error target, 3rd Ref Cell (mV)	5.50	1.10
Display		

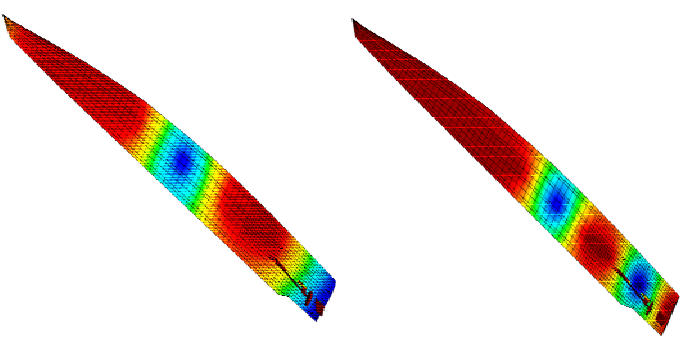

Table 23: Results obtained using the 1st, the 2nd, the 3rd and the 4th references cell as target values and two different sets of arrays.

Four reference cells

	7 Coating sensors	**12 Coating sensors**
Iterations	5	5
Objective function (mV^2)	530.41	242.42
Number of references in the constraints	0/4	0/4
SURFACE REF1: Potential (mV)	–856.0	–851.7
SURFACE REF2: Potential (mV)	–911.8	–907.0
SURFACE REF3: Potential (mV)	–839.4	–835.4
SURFACE REF4: Potential (mV)	–868.4	–870.5
Absolute error target, 1st Ref Cell (mV)	12.60	8.30
Absolute error target, 2nd Ref Cell (mV)	13.80	9.00
Absolute error target, 3rd Ref Cell (mV)	8.50	4.50
Absolute error target, 4th Ref Cell (mV)	10.50	8.40
Display		

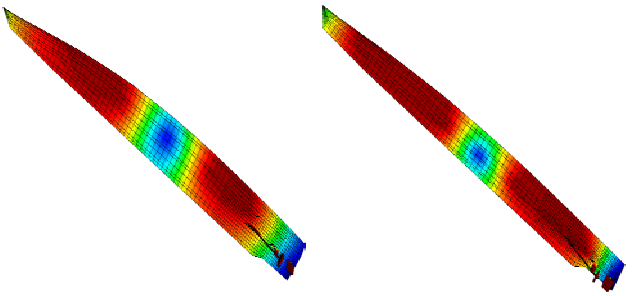

Table 24: Results obtained using the 1st, the 2nd, the 3rd, the 4th and the 5th references cell as target values and two different sets of arrays.

Five reference cells		
	7 Coating sensors	**12 Coating sensors**
Iterations	5	5
Objective function (mV^2)	542.50	297.23
Number of references in the constraints	0/5	0/5
SURFACE REF1: Potential (mV)	–854.2	–851.2
SURFACE REF2: Potential (mV)	–911.1	–907.1
SURFACE REF3: Potential (mV)	–837.5	–835.9
SURFACE REF4: Potential (mV)	–866.8	–869.8
SURFACE REF5: Potential (mV)	–874.7	–875.7
Absolute error target, 1st Ref Cell (mV)	10.80	7.80
Absolute error target, 2nd Ref Cell (mV)	13.10	9.10
Absolute error target, 3rd Ref Cell (mV)	6.60	5.00
Absolute error target, 4th Ref Cell (mV)	12.10	9.10
Absolute error target, 5th Ref Cell (mV)	7.80	6.80
Display		

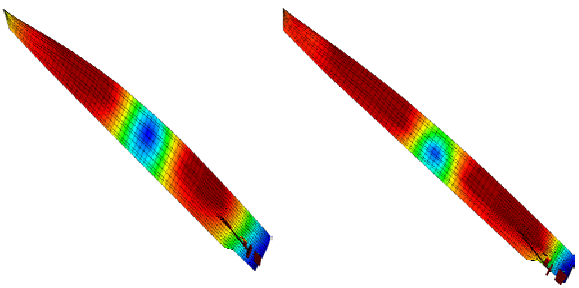

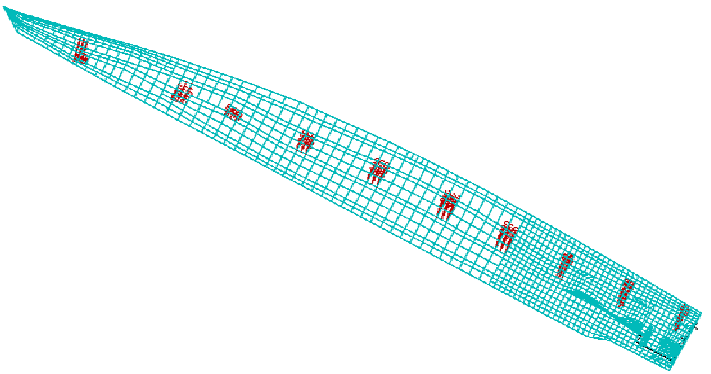

Figure 11: Ten coating sensors distribution on the surface of the frigate.

1.7 Summary

Two models have been analysed, a cylinder model and a frigate model. Both of them had three damaged areas on their surfaces. A compact radial basis function was employed since it becomes zero when the range is exceeded and, therefore, the damaged areas can be detected with respect to the coating area [8].

The objective function increases its value with the number of reference cells, since the distribution of the coating sensors and the interpolation does not exactly represent the real geometry of the damaged areas. This also results in the constraints not being satisfied when the number of reference cells increases. This would imply that the potential tolerance on the constraints should be increased as the number of reference cells increases. However, the solution has been found to converge (*i.e*. becomes accurate) as the number of reference cells increases in all the tests. There is a threshold above which the damage is effectively detected

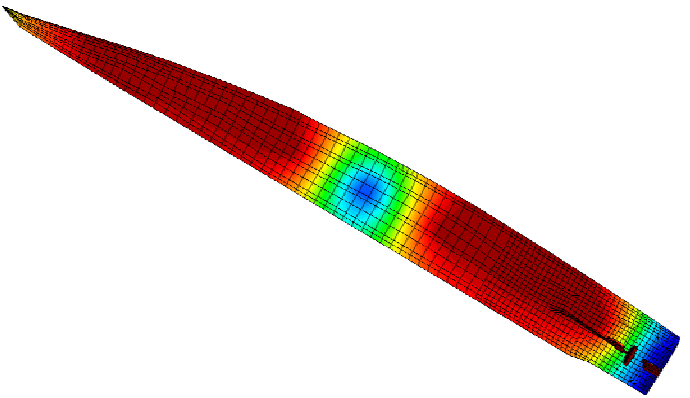

Figure 12: Prediction of the coating using five reference cells and 10 coating.

when enough reference cells data are provided, despite the constraints not being satisfied.

In general, the fact that the final optimum solution does not satisfy the constraints would be considered a failure of the method. However, experience with the techniques suggests that this is not the case and that the solution found is simply the best available. If the constraints are not satisfied and the targets are not matched, it does not mean that the solution is inaccurate but simply the closest one to the final target possible. Given the number and distribution of the sensors and interpolation method used.

The greater the number of coating sensors, the greater the capability of the optimisation to achieve the conditions imposed (constraints). Consequently, increasing the number of coating sensors makes the difference between the target potential and the final design potential becoming smaller.

1.8 Condition of the damaged areas

Despite the damaged areas found, there is no certain idea of what the condition of these damaged areas is. Knowledge of the current distributed to each one of the areas could indicate which of the areas is in the worse condition.

The prediction of the damaged areas is done by an interpolation method along the surface. Thus, there is no clear idea of the real shapes of these areas and therefore what amount of current is being taken.

Three sink points were placed on the top of each one of the damaged areas of the cylinder model, to try to predict this amount of current. Their currents and positions will be modified by the optimisation to achieve the same objective function (15) and constraints employed up to now. Four reference cells data were used in this experiment and the range of constraints are shown in the table 25.

None of the surfaces were in the constraints range by the end of the optimisation since the sinks employed could not emulate the real situation of the damaged areas.

The final positions of these three sink points are shown in fig. 13. The results indicate that the damaged areas predicted previously are confirmed by the sinks.

Table 25: Summary of results obtained when four reference cells were used as target value and 3 movable sinks to emulate the coating.

		Target	Constraints	% out target
Objective function	4134.82			
Number of references in the constraints	1/4			
SURFACE REF1: Potential	–829.2	–773.9	–770, –777	7.15
SURFACE REF2: Potential	–774.7	–770.3	–765, –775	0.57
SURFACE REF3: Potential	–784.0	–758.0	–755, –762	3.43
SURFACE REF4: Potential	–848.4	–867.8	–864, –870	–2.24

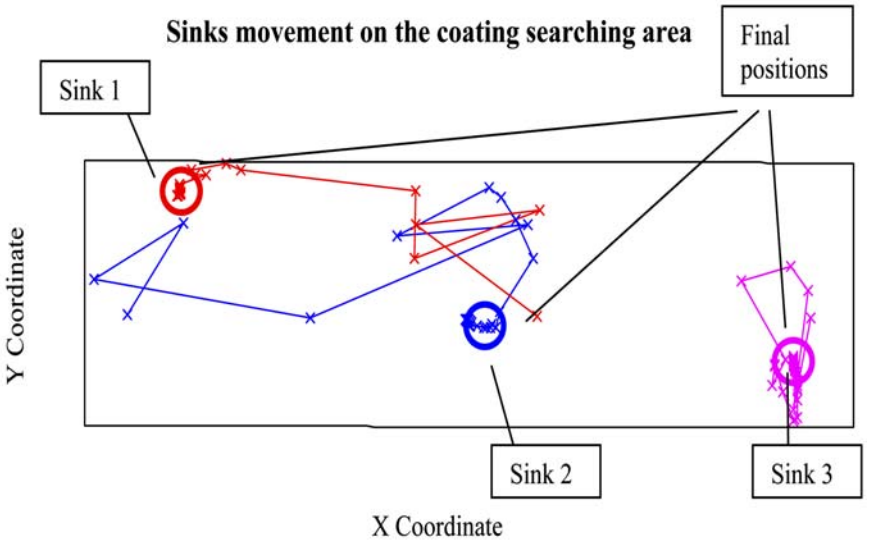

Figure 13: Final positions of the sink points along the search area.

The total current taken by the sinks after the optimisation is similar to the real total current taken by the damaged areas, with an error of 10.3%. However, the currents taken by each of the sinks do not follow the trend of the real current taken by the damaged areas (table 26). This is mainly due to the size and shape of the damaged areas and the difficulty to emulate them with the sink points.

These results could suggest the idea of using the information of the internal points underneath the cylinder to improve the prediction of the real distribution of current on the cylinder surface.

1.9 Condition of the damaged areas from UEP data

Data of the UEP (under electric potential) at 20m from the cylinder are provided. Three sinks have to be moved over the cylinder surface to confirm the positions previously predicted and predict the current taken by each one of the damaged

Table 26: Comparison between the real current taken by the damaged areas and the ones taken by the movable sinks when four reference cells were used.

	Current taken after optimisation (mA)	Real Current taken (mA)	% error
Sink 1	−11059.6	−5109.1	116.47
Sink 2	−2790.0	−8741.7	−68.08
Sink 3	−8756.8	−6650.1	31.68
Total	−22606.3	−20500.9	10.27

areas. The sum of least squares of the current densities with respect to the target values measured at the internal points are to be taken as objective function (18).

– Minimise the summation of the least squares of the components of the signature at the sensors beneath the vessel.

$$\mathrm{Obj}_2 = \sum\left(\mathrm{I}_{\mathrm{X}_{\mathrm{target}_i}} - \mathrm{I}_{\mathrm{X}_{\mathrm{computed}_i}}\right)^2 + \sum\left(\mathrm{I}_{\mathrm{Y}_{\mathrm{target}_i}} - \mathrm{I}_{\mathrm{Y}_{\mathrm{computed}_i}}\right)^2 + \sum\left(\mathrm{I}_{\mathrm{Z}_{\mathrm{target}_i}} - \mathrm{I}_{\mathrm{Z}_{\mathrm{computed}_i}}\right)^2 \tag{18}$$

Where:

$\mathrm{I}_{\mathrm{X}_{\mathrm{target}_i}}$ is the X component of the target current density.

$\mathrm{I}_{\mathrm{Y}_{\mathrm{target}_i}}$ is the Y component of the target current density.

$\mathrm{I}_{\mathrm{Z}_{\mathrm{target}_i}}$ is the Z component of the target current density.

$\mathrm{I}_{\mathrm{X}_{\mathrm{computed}_i}}$ is the X component of the computed current density.

$\mathrm{I}_{\mathrm{Y}_{\mathrm{computed}_i}}$ is the Y component of the computed current density.

$\mathrm{I}_{\mathrm{Zcomputed}_i}$ is the Z component of the computed current density.

Two experiments were carried out: one considering the potential range at the reference cells, constraints; and a second one without considering the potential range at the reference cells (no constraints).

The optimisation will attempt to match the computed electric signature of the cylinder to the target one.

1.9.1 Without considering the reference cells

Three sink points were placed on the cylinder surface. Only the information related to the UEP is available, this is to say that just the current density in the three components of the electric field is available at a distance from the cylinder.

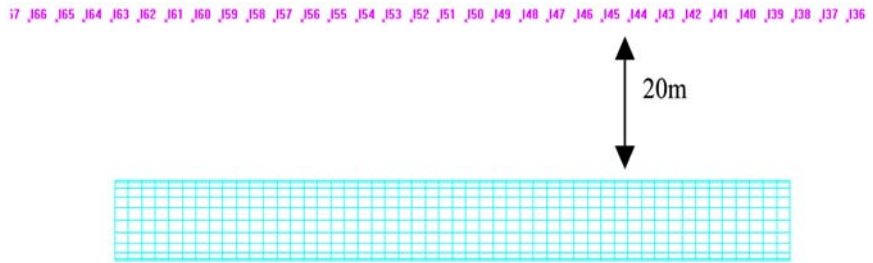

Figure 14: Internal points placed 20m from the cylinder.

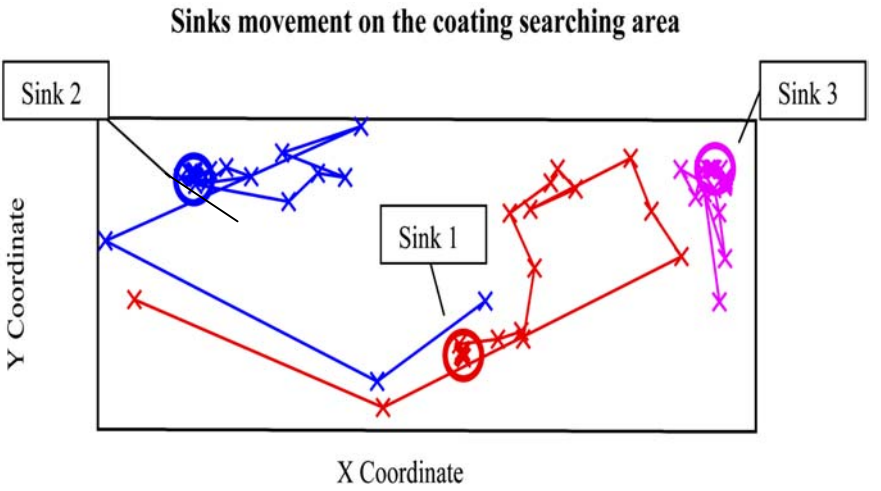

Figure 15: Final position of the sink points by using the UEP.

After the optimisation, the UEP computed has matched the target UEP. The final positions of these three sink points are shown in fig. 15. The results indicate that the damaged areas previously predicted are confirmed by the sinks.

The total current taken by the sinks after the optimisation differs by 29.2% with respect to the real total current taken by the damaged areas. In addition, the current taken by the sinks for the final design do not follow the trend of real current taken by the damaged areas as is shown in table 27. This confirms the hypothesis obtained in previous experiments, the sink points do not properly emulate the real size and shape of the damaged areas.

1.9.2 UEP and reference cells

In this case, not only the information related to the UEP is available but also the information related to the reference cells. A small potential range is set as constraints at the position where reference cells are located.

Table 27: Comparison between the real current taken by the damaged areas and the ones taken by the movable sinks when the UEP was used.

	Current taken after optimisation (mA)	Real Current taken (mA)	% error
Sink 1	–6577.1	–5109.1	28.73
Sink 2	–6301.19	–8741.7	–27.92
Sink 3	–13611.2	–6650.1	104.68
Total	–26489.5	–20500.9	29.21

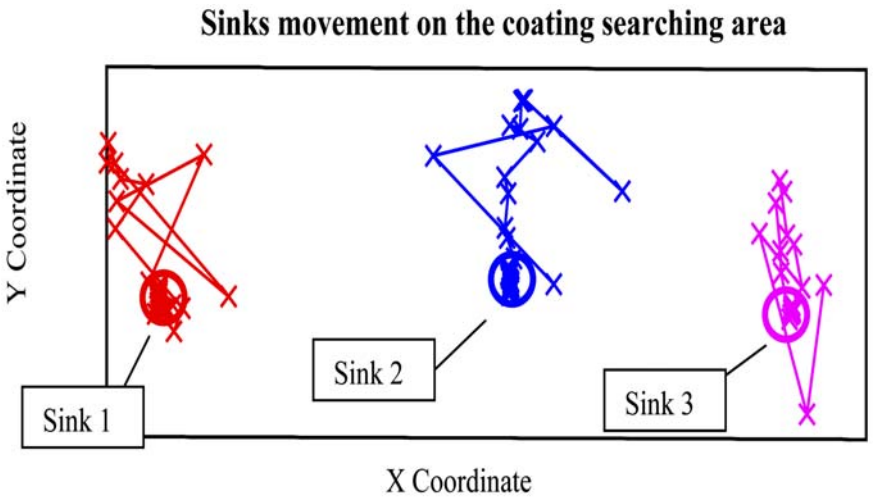

Figure 16: Final position of the sink points by using the UEP.

The optimisation will try to match the target UEP, keeping the potential of the reference cells within a small range around the measured value, smaller than 1%.

After the optimisation, the UEP has matched the target UEP.

The final positions of these three sink points are shown in fig. 16. As before, the results indicate that the damaged areas predicted previously are confirmed by the sinks.

The total current taken by the sinks after the optimisation is similar to the real total current taken by the damaged areas, with an error of 10.41% (table 28). On this occasion, the current taken by the sinks shows a major approach to the real taken current. The smallest damaged area, where the *sink 1* is placed, has been highlighted in this experiment. The results prove that with information about the UEP and potential measures at the reference cells an accurate prediction of the

Table 28: Comparison between the real current taken by the damaged areas and the ones taken by the movable sinks when the UEP and the reference cells potential were used.

	Current taken after optimisation (mA)	Real Current taken (mA)	% error
Sink 1	–5091.9	–5109.1	–0.34
Sink 2	–7884.9	–8741.7	–9.80
Sink 3	–9658.3	–6650.1	45.24
Total	–22635.1	–20500.9	10.41

current taken by the damaged areas could be achieved, despite the sink points not properly emulating the real size and shape of the damaged areas.

1.10 Three closest coating sensors, 4 reference cells

Two interpolation methods were considered to analyse the coating problem state, radial basis function and the three closest coating sensors. Up to now, the radial basis function has been the interpolation method studied in this work. The three closest coating sensors were also analysed in the frigate model with 5 reference cells (fig. 10).

An array of 26 coating sensors was placed on the frigate surface model (fig. 17). A triangular distribution of the coating sensors was considered to be the most suitable since the three closest sensors will be employed to interpolate the coating in the in-between spaces.

Figure 18 shows that damaged areas are reasonably predicted. However, this interpolation method was not considered as effective as the radial basis function since the solution depends on the correct distribution of the coating sensors. To obtain accurate results a fine triangular distribution of the coating sensors could become necessary.

1.11 Polarisation curve of the underlying material

Three polarisation curves were employed to represent different coating states of the surface. They were created by scaling the bare steel surface (fully uncoated) polarisation properties to obtain the 90% bare steel curve and the fully coated curve (fig. 19). Some tests were performed in order to test the difference

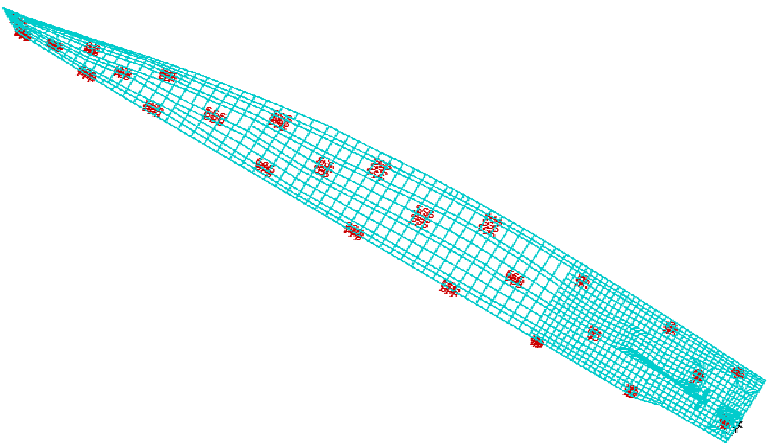

Figure 17: Coating sensors distribution on the prediction surface to study the three closest interpolation method.

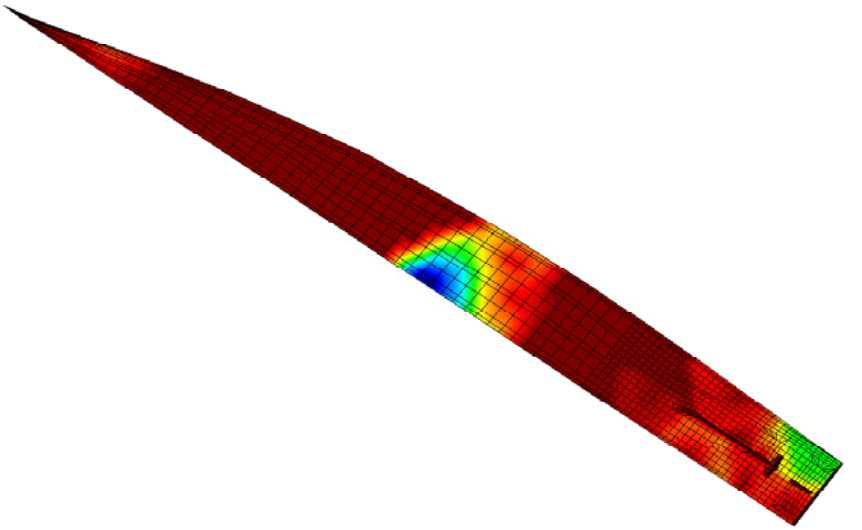

Figure 18: Prediction of the coating using five reference cells, 26 coating sensors and the three closest coating sensors as method of interpolation.

between using the real polarisation curve and a linear approximation. Figure 20 shows the real polarisation curve and a linear polarisation curve with only two

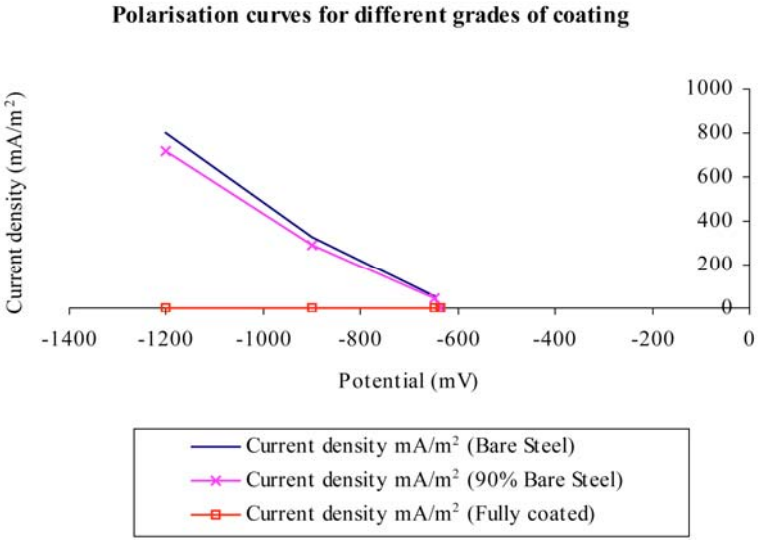

Figure 19: Polarisation curves for different grades of coating and underlying steel.

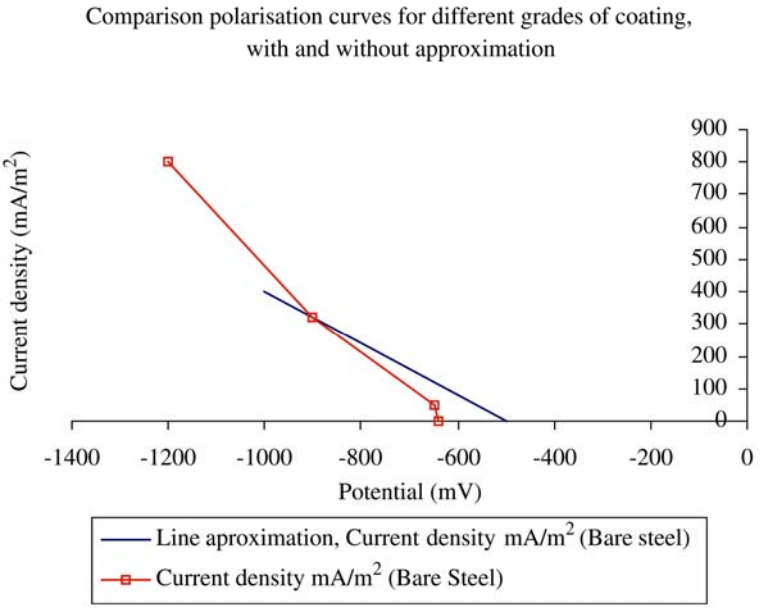

Figure 20: Comparison between the line approximation to bare steel and the real polarisation data.

points, (–500mV, 0mA/m^2) and (–1000mV, 400mA/m^2) for bare steel in sea water.

The coating state was predicted using a line which emulates bare steel and another line with current near 0mA, which emulates the fully coated state. Five reference cells were used (fig. 10) as target values and the set of twelve coating sensors shown in fig. 9. The results obtained predicted the three damaged areas in the approximate correct position (fig. 21) as when real polarisation data were used (table 24).

1.12 Concluding remarks

The prediction of the position of the damaged areas on the surface of a frigate model has been achieved by using the potential measurements at reference cells on the structure.

In spite of being an approximation to the real state of the coating, the RBFs or the three closest sensors enable the location of the damage to be predicted.

A minimum number of potential measurements are necessary to predict the position of the damaged areas otherwise the prediction will not be accurate enough and only some of the damaged areas will be revealed. However, an increase in the number of coating sensors can improve the prediction from the same target data.

Data from the corrosion related electric and magnetic fields can also be employed to identify the condition of a vessel.

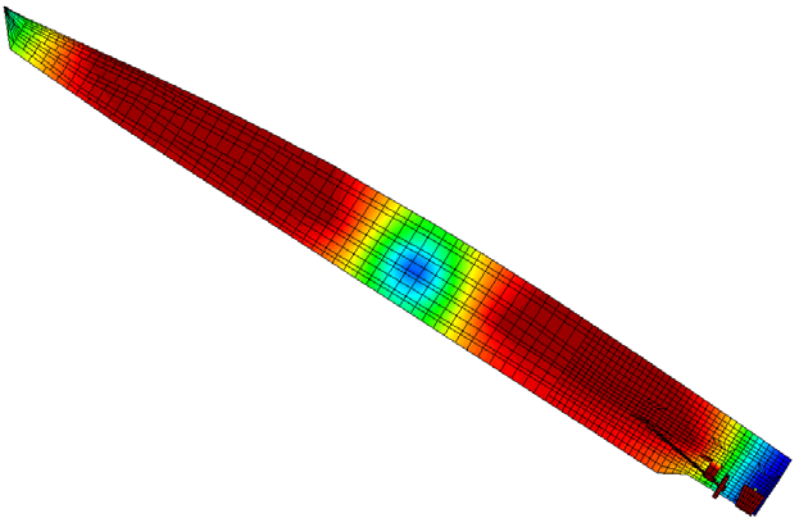

Figure 21: Prediction of the coating of the frigate by using five reference cells, 12 coating sensors and approximate polarisation data.

In the cases tested it was found that a linear approximation to the polarisation data (*i.e.* a curve which roughly represents the behaviour of the underlying materials) was sufficient to predict the location of the damage.

The methods presented could form the basis of a condition monitoring system or improved control system for CP systems.

In addition, the corrosion related electric and magnetic fields were also employed to identify the condition of the vessel.

The electric field and the potential measurements on the vessel can provide, with reasonable accuracy, the position and condition of the damaged areas.

Further testing is required on real shipboard data to validate the techniques further and draw up guidelines for the number of sensors and reference cells required.

References

[1] Santana Diaz, E. & Adey, R., Optimisation of the performance of an ICCP system by changing current supplied and position of the anode, *Boundary Elements Methods* **24** Conference, Sintra, Portugal, 2002.

[2] Santana Diaz, E., Adey, R., Baynham, J. & Pei, Y.H., Optimisation of ICCP systems to minimise electric signatures, Marelec conference 2001, Sweden, 2001.

[3] Santana Diaz, E. & Adey, R., A Computational Environment for the Optimisation of CP system Performance and Signatures, WarshipCP Conference, Royal Military College of Science in Shrivenham, Cranfield University, United Kingdom, 2001.

[4] Rawlins, R.G., Davidson, S.J. & Wilkinson, P.B., Aspects of corrosion related magnetic (CRM) signature management, Wembley Conference Centre, London, UK, 1998, 237–241.
[5] Rawlins, R.G., Davidson, S.J. & Wilkinson, P.B., Aspects of corrosion related magnetic (CRM) signature management, Wembley Conference Centre, London, UK, pp. 237–241 (1998).
[6] Aoki, S., Amaya, K. & Gouka, K., Optimal cathodic protection of ship, In *Boundary Element Technology XI,* ed. R.C. Ertekin, C.A. Brebbia, M. Tanaka & R. Shaw. pp. 345–356 (1996).
[7] Diaz, E.S. & Adey, R., Corrosion optimisation using boundary elements, *Boundary Elements Communications;* **12**, N.1, 2001; 12–25.
[8] Leitao, V.M.A., & Tiago, C.M., The use of radial basis functions for one-dimensional structural analysis problems, *Boundary Elements XXIV*, eds. C.A. Brebbia, A. Taden & V. Popov. pp. 165–179 (1996).
[9] Vanderplaats, G.N., DOT/DOC Users Manual, Vanderplaats, Miura and Associates, 1993.
[10] Castillo, E., Conejo, A.J., Pedregal, P., García, R., & Alguacil, N., *Building and solving mathematical programming models in engineering and science*, Wiley Interscience, 2001; 190–207.
[11] Morgan, John, *Cathodic Protection*. National Association of Corrosion Engineers, NACE. (1987).